

Supplementary information on the article:

## Interplay of thermalization and strong disorder: Wave turbulence theory, numerical simulations, and experiments in multimode optical fibers

Nicolas Berti<sup>1</sup>, Kilian Baudin<sup>1</sup>, Adrien Fusaro<sup>2</sup>, Guy Millot<sup>1,3</sup>, Antonio Picozzi<sup>1</sup>, Josselin Garnier<sup>4</sup>

<sup>1</sup> Laboratoire Interdisciplinaire Carnot de Bourgogne,

CNRS, Université Bourgogne Franche-Comté, Dijon, France

<sup>2</sup> CEA, DAM, DIF, F-91297 Arpajon Cedex, France

<sup>3</sup> Institut Universitaire de France (IUF), 1 rue Descartes, 75005 Paris, France and

<sup>4</sup> CMAP, CNRS, Ecole Polytechnique, Institut Polytechnique de Paris, 91128 Palaiseau Cedex, France

### I. DERIVATION OF THE KINETIC EQ.(4)

#### A. Primary asymptotics

The starting point is the NLS Eq.(1) (main text) written in the mode basis, i.e., Eq.(2) (main text). We consider the regime where linear propagation dominates over disorder, which in turn dominates over the nonlinearity. Accordingly, we introduce a small dimensionless parameter  $\varepsilon$  and we consider the regime  $\beta_j \rightarrow \beta_j, \mathbf{C} \rightarrow \varepsilon \mathbf{C}, \gamma \rightarrow \varepsilon^2 \gamma$ . For propagation distances of order  $\varepsilon^{-2}$ , the rescaled mode amplitudes  $a_j^\varepsilon(z) = a_j(z/\varepsilon^2)$  satisfy

$$\partial_z a_j^\varepsilon = -i \frac{\beta_j}{\varepsilon^2} a_j^\varepsilon + i\gamma \sum_{l,m,n=0}^{M-1} Q_{jlmn} a_l^\varepsilon a_m^\varepsilon \overline{a_n^\varepsilon} - \frac{i}{\varepsilon} \sum_{l=0}^{M-1} C_{jl} \left(\frac{z}{\varepsilon^2}\right) a_l^\varepsilon,$$

where the bar stands for complex conjugation. We set  $c_j^\varepsilon(z) = a_j^\varepsilon(z) \exp(i \frac{\beta_j}{\varepsilon^2} z)$ . The amplitudes  $c_j^\varepsilon(z)$  satisfy:

$$\begin{aligned} \partial_z c_j^\varepsilon = & i\gamma \sum_{l,m,n=0}^{M-1} Q_{jlmn} c_l^\varepsilon c_m^\varepsilon \overline{c_n^\varepsilon} \exp\left(i \frac{\beta_j - \beta_l - \beta_m + \beta_n}{\varepsilon^2} z\right) \\ & - \frac{i}{\varepsilon} \sum_{l=0}^{M-1} C_{jl} \left(\frac{z}{\varepsilon^2}\right) c_l^\varepsilon \exp\left(i \frac{\beta_j - \beta_l}{\varepsilon^2} z\right). \end{aligned} \quad (S1)$$

This is the usual diffusion approximation framework [1]. We get the following result.

**Proposition I.1** *The random process  $(c_j^\varepsilon(z))_{j=0}^{M-1}$  converges in distribution in  $\mathcal{C}^0([0, \infty), \mathbb{C}^M)$ , the space of continuous functions from  $[0, \infty)$  to  $\mathbb{C}^M$ , to the Markov process  $(c_j(z))_{j=0}^{M-1}$  with infinitesimal generator  $\mathcal{L}$ :*

$$\mathcal{L} = \mathcal{L}_1 + \mathcal{L}_2 + \mathcal{L}_3 + \mathcal{L}_4 + \mathcal{L}_5, \quad (S2)$$

with

$$\begin{aligned} \mathcal{L}_1 = & \frac{1}{2} \sum_{j,l=0,j \neq l}^{M-1} \Gamma_{jl}^{\text{OD}} \left( c_j \overline{c_l} \partial_{c_l} \partial_{\overline{c_l}} + c_l \overline{c_j} \partial_{c_j} \partial_{\overline{c_j}} \right. \\ & \left. - c_j c_l \partial_{c_j} \partial_{c_l} - \overline{c_j} \overline{c_l} \partial_{\overline{c_j}} \partial_{\overline{c_l}} \right), \\ \mathcal{L}_2 = & \frac{1}{2} \sum_{j,l=0}^{M-1} \Gamma_{jl}^{\text{D}} \left( c_j \overline{c_l} \partial_{c_j} \partial_{\overline{c_l}} + \overline{c_j} c_l \partial_{\overline{c_j}} \partial_{c_l} \right. \\ & \left. - c_j c_l \partial_{c_j} \partial_{c_l} - \overline{c_j} \overline{c_l} \partial_{\overline{c_j}} \partial_{\overline{c_l}} \right), \end{aligned}$$

$$\mathcal{L}_3 = \frac{1}{2} \sum_{j=0}^{M-1} \Gamma_{jj}^{\text{OD}} (c_j \partial_{c_j} + \overline{c_j} \partial_{\overline{c_j}}) + i \hat{\Gamma}_{jj}^{\text{OD}} (c_j \partial_{c_j} - \overline{c_j} \partial_{\overline{c_j}}),$$

$$\mathcal{L}_4 = -\frac{1}{2} \sum_{j=0}^{M-1} \Gamma_{jj}^{\text{D}} (c_j \partial_{c_j} + \overline{c_j} \partial_{\overline{c_j}}),$$

$$\mathcal{L}_5 = i\gamma \sum_{l,m,n=0}^{M-1} \delta_{jlmn}^K Q_{jlmn} (c_l c_m \overline{c_n} \partial_{c_j} - \overline{c_l} \overline{c_m} c_n \partial_{\overline{c_j}}),$$

where  $\delta_{jlmn}^K = \mathbf{1}_{\beta_j - \beta_l - \beta_m + \beta_n = 0}$ . In this definition we use the classical complex derivative: if  $\zeta = \zeta_r + i\zeta_i$ , then  $\partial_\zeta = (1/2)(\partial_{\zeta_r} - i\partial_{\zeta_i})$  and  $\partial_{\overline{\zeta}} = (1/2)(\partial_{\zeta_r} + i\partial_{\zeta_i})$ , and the coefficients of the operator  $\mathcal{L}_k$  ( $k = 1, \dots, 5$ ) are defined for  $j, l = 0, \dots, M-1$ , as follows:

- For all  $j \neq l$ ,  $\Gamma_{jl}$  and  $\hat{\Gamma}_{jl}^{\text{OD}}$  are given by

$$\Gamma_{jl}^{\text{OD}} = 2 \int_0^\infty \mathcal{R}_{jl}(z) \cos((\beta_l - \beta_j)z) dz, \quad (S3)$$

$$\hat{\Gamma}_{jl}^{\text{OD}} = 2 \int_0^\infty \mathcal{R}_{jl}(z) \sin((\beta_l - \beta_j)z) dz, \quad (S4)$$

with  $\mathcal{R}_{jl}(z)$  defined by

$$\begin{aligned} \mathcal{R}_{jl}(z) = & \mathbb{E}[C_{jl}(0)C_{jl}(z)] \\ = & \iint u_j(\mathbf{r}) u_j(\mathbf{r}') \mathbb{E}[\delta V(0, \mathbf{r}) \delta V(z, \mathbf{r}')] u_l(\mathbf{r}) u_l(\mathbf{r}') d\mathbf{r} d\mathbf{r}'. \end{aligned} \quad (S5)$$

- For all  $j, l = 0, \dots, M-1$ :

$$\Gamma_{jl}^{\text{D}} = \int_0^\infty \mathbb{E}[C_{jj}(0)C_{ll}(z)] dz + \int_0^\infty \mathbb{E}[C_{ll}(0)C_{jj}(z)] dz. \quad (S6)$$

- For all  $j = 0, \dots, M-1$ :

$$\Gamma_{jj}^{\text{OD}} = -\sum_{l=0,l \neq j}^{M-1} \Gamma_{jl}^{\text{OD}}, \quad \hat{\Gamma}_{jj}^{\text{OD}} = -\sum_{l=0,l \neq j}^{M-1} \hat{\Gamma}_{jl}^{\text{OD}}. \quad (S7)$$

#### B. Secondary asymptotics

We observe that  $\Gamma^{\text{OD}}$  and  $\hat{\Gamma}^{\text{OD}}$  depend on the power spectral density of the random index perturbation evaluated at the difference of distinct frequencies  $\beta_j - \beta_l$ , while  $\Gamma^{\text{D}}$  depends on the power spectral density of the index perturbation evaluated at zero-frequency. Therefore, when  $L_{lin} =$

$1/\beta_0 \ll \ell_c$ , then  $\Gamma^D$  is larger than  $\Gamma^{OD}, \hat{\Gamma}^{OD}$ . We consider this regime by introducing a small dimensionless parameter  $\eta$  with  $\Gamma^D \rightarrow \Gamma^D, \Gamma^{OD} \rightarrow \eta^2 \Gamma^{OD}, \hat{\Gamma}^{OD} \rightarrow \eta^2 \hat{\Gamma}^{OD}, \gamma \rightarrow \eta\gamma$ .

For propagation distances of order  $\eta^{-2}$ , we introduce the rescaled mode amplitudes  $\mathbf{c}_j^\eta(z) = \mathbf{c}_j(z/\eta^2)$ . By Proposition I.1 it is a Markov process with infinitesimal generator  $\mathcal{L}^\eta$ :

$$\mathcal{L}^\eta = \mathcal{L}_1 + \eta^{-2} \mathcal{L}_2 + \mathcal{L}_3 + \eta^{-2} \mathcal{L}_4 + \eta^{-1} \mathcal{L}_5, \quad (\text{S8})$$

where the operators  $\mathcal{L}_k$  ( $k = 1, \dots, 5$ ) are given above. By (S8) the second-order moments satisfy for  $j \neq j'$ :

$$\begin{aligned} \partial_z \mathbb{E}[\mathbf{c}_j^\eta \overline{\mathbf{c}_{j'}^\eta}] &= -\frac{1}{2\eta^2} (\Gamma_{jj}^D + \Gamma_{j'j'}^D - 2\Gamma_{jj'}^D) \mathbb{E}[\mathbf{c}_j^\eta \overline{\mathbf{c}_{j'}^\eta}] \\ &+ \frac{1}{2} (\Gamma_{jj}^{OD} + \Gamma_{j'j'}^{OD}) \mathbb{E}[\mathbf{c}_j^\eta \overline{\mathbf{c}_{j'}^\eta}] + \frac{i}{2} (\hat{\Gamma}_{jj}^{OD} - \hat{\Gamma}_{j'j'}^{OD}) \mathbb{E}[\mathbf{c}_j^\eta \overline{\mathbf{c}_{j'}^\eta}] \\ &+ i \frac{\gamma}{\eta} \sum_{l,m,n=0}^{M-1} \delta_{jlmn}^K Q_{jlmn} \mathbb{E}[\mathbf{c}_j^\eta \overline{\mathbf{c}_l^\eta} \mathbf{c}_m^\eta \overline{\mathbf{c}_n^\eta}] \\ &- i \frac{\gamma}{\eta} \sum_{l,m,n=0}^{M-1} \delta_{j'lmn}^K Q_{j'lmn} \mathbb{E}[\mathbf{c}_j^\eta \overline{\mathbf{c}_l^\eta} \mathbf{c}_m^\eta \overline{\mathbf{c}_n^\eta}], \end{aligned}$$

up to negligible terms in  $\eta$ . Note that  $\Gamma_{jj}^D + \Gamma_{j'j'}^D - 2\Gamma_{jj'}^D = \int_{-\infty}^{\infty} \mathbb{E}[(C_{jj}(0) - C_{j'j'}(0))(C_{jj}(z) - C_{j'j'}(z))] dz$  is positive (it is the power spectral density evaluated at 0 frequency of the stationary process  $C_{jj}(z) - C_{j'j'}(z)$  by Bochner's theorem). Therefore  $\mathbb{E}[\mathbf{c}_j^\eta \overline{\mathbf{c}_{j'}^\eta}]$  is exponentially damped and

$$\mathbb{E}[\mathbf{c}_j^\eta \overline{\mathbf{c}_{j'}^\eta}] = O(\eta). \quad (\text{S9})$$

If  $j = j'$ , then the mean square amplitudes  $w_j^\eta(z) = \mathbb{E}[|\mathbf{c}_j^\eta(z)|^2]$  satisfy

$$\begin{aligned} \partial_z w_j^\eta &= \sum_{l=0, l \neq j}^{M-1} \Gamma_{jl}^{OD} (w_l^\eta - w_j^\eta) \\ &- 2 \frac{\gamma}{\eta} \sum_{l,m,n=0}^{M-1} \delta_{jlmn}^K Q_{jlmn} \text{Im} \left\{ \mathbb{E}[\mathbf{c}_j^\eta \overline{\mathbf{c}_l^\eta} \mathbf{c}_m^\eta \overline{\mathbf{c}_n^\eta}] \right\}. \quad (\text{S10}) \end{aligned}$$

By (S8) the fourth-order moments satisfy

$$\begin{aligned} \partial_z \mathbb{E}[\mathbf{c}_j^\eta \overline{\mathbf{c}_l^\eta} \mathbf{c}_m^\eta \overline{\mathbf{c}_n^\eta}] &= -\frac{1}{2\eta^2} G_{jlmn}^D \mathbb{E}[\mathbf{c}_j^\eta \overline{\mathbf{c}_l^\eta} \mathbf{c}_m^\eta \overline{\mathbf{c}_n^\eta}] + i \frac{\gamma}{\eta} Y_{jlmn}^\eta \\ &+ \sum_{j', l', m', n'} M_{jlmn, j'l'm'n'} \mathbb{E}[\mathbf{c}_j^\eta \overline{\mathbf{c}_{l'}^\eta} \mathbf{c}_{m'}^\eta \overline{\mathbf{c}_{n'}^\eta}], \quad (\text{S11}) \end{aligned}$$

up to negligible terms in  $\eta$ . The coefficients  $G_{jlmn}^D$  and the sixth-order moment  $Y_{jlmn}^\eta$  are given by

$$\begin{aligned} G_{jlmn}^D &= \Gamma_{ll}^D + \Gamma_{mm}^D + \Gamma_{nn}^D + \Gamma_{jj}^D + 2\Gamma_{lm}^D - 2\Gamma_{ln}^D \\ &- 2\Gamma_{lj}^D - 2\Gamma_{mn}^D - 2\Gamma_{mj}^D + 2\Gamma_{nj}^D, \quad (\text{S12}) \end{aligned}$$

$$\begin{aligned} Y_{jlmn}^\eta &= \sum_{l', m', n'=0}^{M-1} \delta_{ll'm'n'}^K S_{ll'm'n'} \mathbb{E}[\mathbf{c}_l^\eta \overline{\mathbf{c}_{l'}^\eta} \mathbf{c}_m^\eta \overline{\mathbf{c}_{m'}^\eta} \mathbf{c}_n^\eta \overline{\mathbf{c}_{n'}^\eta} \mathbf{c}_j^\eta] \\ &+ \delta_{ml'm'n'}^K S_{ml'm'n'} \mathbb{E}[\mathbf{c}_l^\eta \overline{\mathbf{c}_{l'}^\eta} \mathbf{c}_m^\eta \overline{\mathbf{c}_{m'}^\eta} \mathbf{c}_n^\eta \overline{\mathbf{c}_{n'}^\eta} \mathbf{c}_j^\eta] \\ &- \delta_{nl'm'n'}^K S_{nl'm'n'} \mathbb{E}[\mathbf{c}_l^\eta \overline{\mathbf{c}_{l'}^\eta} \mathbf{c}_m^\eta \overline{\mathbf{c}_{m'}^\eta} \mathbf{c}_n^\eta \overline{\mathbf{c}_{n'}^\eta} \mathbf{c}_j^\eta] \\ &- \delta_{jl'm'n'}^K Q_{jl'm'n'} \mathbb{E}[\mathbf{c}_l^\eta \overline{\mathbf{c}_{l'}^\eta} \mathbf{c}_m^\eta \overline{\mathbf{c}_{m'}^\eta} \mathbf{c}_n^\eta \overline{\mathbf{c}_{n'}^\eta}], \quad (\text{S13}) \end{aligned}$$

up to negligible terms in  $\eta$ . The tensor  $M_{jlmn, j'l'm'n'}$  involves the coefficients  $\Gamma^{OD}$  and  $\hat{\Gamma}^{OD}$ . Note that we have  $G_{jlmn}^D = \int_{-\infty}^{\infty} \mathbb{E}[(Cu(0) + C_{mm}(0) - C_{nn}(0) - C_{jj}(0))(Cu(z) + C_{mm}(z) - C_{nn}(z) - C_{jj}(z))] dz \geq 0$ . Therefore, we find from (S11) that

$$\mathbb{E}[\mathbf{c}_j^\eta \overline{\mathbf{c}_l^\eta} \mathbf{c}_m^\eta \overline{\mathbf{c}_n^\eta}] = \frac{2i\eta\gamma}{G_{jlmn}^D} Y_{jlmn}^\eta + O(\eta^2).$$

By substituting into (S10) and by using Isserlis formula for the sixth-order moments that appear in the expression (S13) of  $Y_{jlmn}^\eta$  we obtain the kinetic Eq.(4) in the main text:

$$\begin{aligned} \partial_z w_j^\eta &= \sum_{l=0, l \neq j}^{M-1} \Gamma_{jl}^{OD} (w_l^\eta - w_j^\eta) \\ &+ 8\gamma^2 \sum_{l,m,n=0}^{M-1} \frac{\delta_{jlmn}^K Q_{jlmn}^2}{G_{jlmn}^D} (w_l^\eta w_m^\eta w_j^\eta + w_l^\eta w_m^\eta w_n^\eta \\ &- w_j^\eta w_n^\eta w_m^\eta - w_j^\eta w_n^\eta w_l^\eta). \quad (\text{S14}) \end{aligned}$$

The second term in (S14) has a form analogous to the conventional collision term of the wave turbulence kinetic equation [2]. Exploiting the invariances properties of the tensors  $Q_{jlmn}$  and  $G_{jlmn}^D$ , as well as the property  $G_{jlmn}^D \geq 0$ , it can be shown that the collision term conserves the particle number  $N = \sum_j w_j$ , the energy  $E = \sum_j \beta_j w_j$ , and exhibits a  $H$ -theorem of entropy growth  $\partial_z S(z) \geq 0$ , where the nonequilibrium entropy reads  $S(z) = \sum_j \log[w_j(z)]$  (note that, for simplicity we omitted to write the superscript  $\eta$ ). The entropy growth saturates at thermal equilibrium. The RJ equilibrium distribution that maximizes the entropy  $S[w_j]$ , under the constraints that  $N$  and  $E$  are conserved, reads

$$w_j^{\text{RJ}} = T/(\beta_j - \mu), \quad (\text{S15})$$

where  $1/T$  and  $-\mu/T$  are the Lagrange multipliers associated to the conservation of  $E$  and  $N$ . There is a one to one relation between the pair  $(N, E)$  and  $(T, \mu)$ : The values of the conserved quantities  $(N, E)$  determine uniquely  $(T, \mu)$ , and thus the RJ equilibrium (S15).

### C. Degenerate modes

In this section we assume that the modes may be degenerate. The detailed derivation of the kinetic equation accounting for mode degeneracy is cumbersome and will be reported elsewhere. Here we report the main results.

There are  $G$  distinct wavenumbers:

$$\{\beta^{(g)}, g = 1, \dots, G\},$$

and the mode indices can be partitioned into  $G$  groups  $\mathcal{G}^{(g)}$ ,  $g = 1, \dots, G$ :

$$\mathcal{G}^{(g)} = \{p = 1, \dots, N, \beta_p = \beta^{(g)}\}.$$

We obtain the kinetic equation

$$\begin{aligned} \partial_z w^{(g)} &= 8\gamma^2 \sum_{g_1, g_2, g_3=1}^G \delta^{(gg_1 g_2 g_3)} q^{(gg_1 g_2 g_3)} (w^{(g)} w^{(g_3)} w^{(g_2)} \\ &+ w^{(g)} w^{(g_3)} w^{(g_1)} - w^{(g_1)} w^{(g_2)} w^{(g)} - w^{(g_1)} w^{(g_2)} w^{(g_3)}), \end{aligned}$$

where

$$q^{(gg_1g_2g_3)} = \frac{1}{|\mathcal{G}^{(g)}|} \sum_{j \in \mathcal{G}^{(g)}, l \in \mathcal{G}^{(g_1)}, m \in \mathcal{G}^{(g_2)}, n \in \mathcal{G}^{(g_3)}} Q_{jlmn} Q_{jlmn}^{(gg_1g_2g_3)}$$

where

$$\begin{aligned} \mathbf{Q}^{(gg_1g_2g_3)} &= (Q_{jlmn}^{(gg_1g_2g_3)})_{j \in \mathcal{G}^{(g)}, l \in \mathcal{G}^{(g_1)}, m \in \mathcal{G}^{(g_2)}, n \in \mathcal{G}^{(g_3)}} \\ &= (\mathbf{M}^{(gg_1g_2g_3)})^{-1} ((Q_{jlmn})_{j \in \mathcal{G}^{(g)}, l \in \mathcal{G}^{(g_1)}, m \in \mathcal{G}^{(g_2)}, n \in \mathcal{G}^{(g_3)}}). \end{aligned}$$

The tensor  $\mathbf{M}^{(gg_1g_2g_3)}$  (seen as a  $q \times q$  matrix with  $q = |\mathcal{G}^{(g)}||\mathcal{G}^{(g_1)}||\mathcal{G}^{(g_2)}||\mathcal{G}^{(g_3)}|$ ) is given by

$$\begin{aligned} &\sum_{j' \in \mathcal{G}^{(g)}, l' \in \mathcal{G}^{(g_1)}, m' \in \mathcal{G}^{(g_2)}, n' \in \mathcal{G}^{(g_3)}} M_{jlmn, j'l'm'n'}^{(gg_1g_2g_3)} \\ &= \sum_{l' \in \mathcal{G}^{(g_1)}, m' \in \mathcal{G}^{(g_2)}} 2\gamma_{l'm'm'} w_{j'l'm'n'} \\ &+ \sum_{n' \in \mathcal{G}^{(g_3)}, j' \in \mathcal{G}^{(g)}} 2\gamma_{nn'jj'} w_{j'l'mn'} \\ &- \sum_{l' \in \mathcal{G}^{(g_1)}, n' \in \mathcal{G}^{(g_3)}} 2\gamma_{l'l'nn'} w_{j'l'mn'} \\ &- \sum_{l' \in \mathcal{G}^{(g_1)}, j' \in \mathcal{G}^{(g)}} 2\gamma_{l'l'jj'} w_{j'l'mn'} \\ &- \sum_{m' \in \mathcal{G}^{(g_2)}, n' \in \mathcal{G}^{(g_3)}} 2\gamma_{mm'n'n'} w_{jlm'n'} \\ &- \sum_{m' \in \mathcal{G}^{(g_2)}, j' \in \mathcal{G}^{(g)}} 2\gamma_{mm'jj'} w_{j'l'mn'} \\ &+ \sum_{l', l'' \in \mathcal{G}^{(g_1)}} \gamma_{l'l'l''} w_{j'l'mn'} + \sum_{m', m'' \in \mathcal{G}^{(g_2)}} \gamma_{m'm'm''} w_{jlm'n'} \\ &+ \sum_{n', n'' \in \mathcal{G}^{(g_3)}} \gamma_{n'n'n''} w_{jlmn'} + \sum_{j', j'' \in \mathcal{G}^{(g)}} \gamma_{j'j'j''} w_{j'l'mn'}. \end{aligned}$$

where

$$\gamma_{pq p'q'} = 2 \int_0^\infty \mathbb{E}[C_{pq}(z)C_{p'q'}(0)] e^{i(\beta_p - \beta_q)z} dz.$$

## D. Numerical simulations

*Implementation of disorder:* To implement the disorder in the simulations of the NLS Eq.(2) (main text), we considered an *exact discretization* of the Ornstein-Uhlenbeck process. The propagation axis is divided in intervals with deterministic lengths  $\Delta z$ , with  $\Delta z < \ell_c$ . The random function  $\mu(z)$  is stepwise constant over each elementary interval  $z \in [k\Delta z, (k+1)\Delta z)$ , where  $\mu_0 \sim \mathcal{N}(0, \sigma^2/2)$  denotes the Gaussian distribution,  $\mu_k = \sqrt{1 - 2\Delta z/\ell_c} \mu_{k-1} + \sqrt{2\Delta z/\ell_c} \mathcal{N}(0, \sigma^2/2)$ , with  $\mathcal{N}(0, \sigma^2/2)$  all independent and identically distributed.

*Model of disorder:* We have considered in the numerical simulations an elliptical parabolic potential  $V(\mathbf{x}) = q_x x^2 + q_y y^2$ , with  $u_{p_x, p_y}(x, y) = \sqrt{\kappa_x \kappa_y} (\pi p_x! p_y! 2^{2p_x + 2p_y})^{-1/2} H_{p_x}(\kappa_x x) H_{p_y}(\kappa_y y) \exp[-(\kappa_x^2 x^2 + \kappa_y^2 y^2)/2]$  the normalized Hermite-Gaussian functions with corresponding eigenvalues  $\beta_p = \beta_{p_x, p_y} =$

$\beta_{0x}(p_x + 1/2) + \beta_{0y}(p_y + 1/2)$ , with  $\kappa_x = (q_x/\alpha)^{1/4}$ ,  $\kappa_y = (q_y/\alpha)^{1/4}$ ,  $\beta_{0x} = 2\sqrt{\alpha q_x}$ ,  $\beta_{0y} = 2\sqrt{\alpha q_y}$ , and the radii of the fundamental mode  $r_{0x} = 1/\kappa_x = \sqrt{2\alpha/\beta_{0x}}$ ,  $r_{0y} = 1/\kappa_y = \sqrt{2\alpha/\beta_{0y}}$ .

We have considered the following form of model of disorder:  $\delta V(\mathbf{x}, z) = \mu(z) \cos(\kappa_x b_x x) \cos(\kappa_y b_y y)$ , with  $\mathbb{E}[\mu(0)\mu(z)] = \sigma^2 f(z)$ ,  $f(z) = \exp(-|z|/\ell_c)$ . The advantage of this model is that the matrices  $\mathbf{C}, \mathbf{\Gamma}^D, \mathbf{\Gamma}^{OD}$  can be computed in analytical form. We have  $C_{nk}(z) = \mu(z) C_{n_x k_x}^0 C_{n_y k_y}^0 = \mu(z) \int u_{n_x}(x) \cos(\kappa_x b_x x) u_{k_x}(x) dx \int u_{n_y}(y) \cos(\kappa_y b_y y) u_{k_y}(y) dy$ . Then we have for  $j_x, j_y, l_x, l_y \geq 0$ :  $C_{j, j+2l} = \mu(z) C_{j_x, j_x+2l_x}^0 C_{j_y, j_y+2l_y}^0$  where we denote for  $s = x$  or  $s = y$ :

$$C_{j_s, j_s+2l_s}^0 = (-1)^{l_s} b_s^{2l_s} \exp(-b_s^2/4) L_{j_s}^{2l_s}(b_s^2/2) \frac{\sqrt{j_s!/(j_s+2l_s)!}}{2^{l_s}}$$

and  $C_{j_s, j_s+2l_s+1}^0 = 0$ , where  $L_j^l$  is the generalized Laguerre polynomial [3, formula 7.388.7]. In particular  $C_{j_s, j_s}^0 = \exp(-b_s^2/4) L_{j_s}^{2j_s}(b_s^2/2)$ , where  $L_j$  is the Laguerre polynomial. For  $j_x, j_y, l_x, l_y \geq 0$ , we have  $\Gamma_{jl}^D = 2\sigma^2 \ell_c C_{j_x, j_x}^0 C_{j_y, j_y}^0 C_{l_x, l_x}^0 C_{l_y, l_y}^0$ .

For  $n_x, k_x, n_y, k_y \geq 0$  we obtain:

$$\Gamma_{n,k}^{OD} = \frac{2\sigma^2 \ell_c \mathcal{R}_{n_x, k_x}^0 \mathcal{R}_{n_y, k_y}^0}{1 + \ell_c^2 [\beta_{0x}(n_x - k_x) + \beta_{0y}(n_y - k_y)]^2},$$

where  $\mathcal{R}_{j_s, j_s+2l_s+1}^0 = 0$  and

$$\mathcal{R}_{j_s, j_s+2l_s}^0 = b_s^{4l_s} \exp(-b_s^2/2) L_{j_s}^{2l_s}(b_s^2/2)^2 (j_s!/(j_s+2l_s)!) 2^{-2l_s}.$$

In order to avoid high values of  $\Gamma_{n,k}^{OD}$ , we have considered an irrational ratio  $\beta_{0x}/\beta_{0y} = \sqrt{2}$ , so that  $\beta_{0x}(n_x - k_x) + \beta_{0y}(n_y - k_y) \neq 0$ . Parameters are  $(b_x = 0.4, b_y = 0.5)$  in Figs. 1-2, and  $(b_x = 0.4, b_y = 0.3)$  in Fig. 3. In all cases we considered  $M = 46$  modes. The value of  $L_{nl} = 1/(\gamma N/A_{eff}^0)$  in the simulations is computed by considering that all the power  $N$  is in the fundamental mode of effective area  $A_{eff}^0 = 1/\int |u_0|^4(\mathbf{r}) d\mathbf{r}$ .

## II. EXPERIMENTAL METHODS

**1) Setup:** The experimental setup has been described in detail in Ref.[4]. Here we summarize the main characteristics. The source is a Nd:YAG laser delivering subnanosecond pulses (400ps) at  $\lambda_0 = 1064$  nm. We control the power with a half-wave plate and a polarizer. The laser beam was collimated and passed through a glass diffuser plate placed in the vicinity of the Fourier plane of a 4f-optical system. The beam was launched into the MMF. The near-field (NF) and far-field (FF) intensity distributions are measured at the fiber output following the procedure of Ref.[4]. We used a 12m-long graded-index MMF whose refractive index profile exhibits a parabolic shape in the fiber core with a maximum core index (at the center) of  $n_{co} = 1.470$  and  $n_{cl} = 1.457$  for the cladding at the pump wavelength of 1064nm (numerical aperture NA=0.195, fiber radius  $R = 26\mu\text{m}$ ,  $\beta_0 \approx$

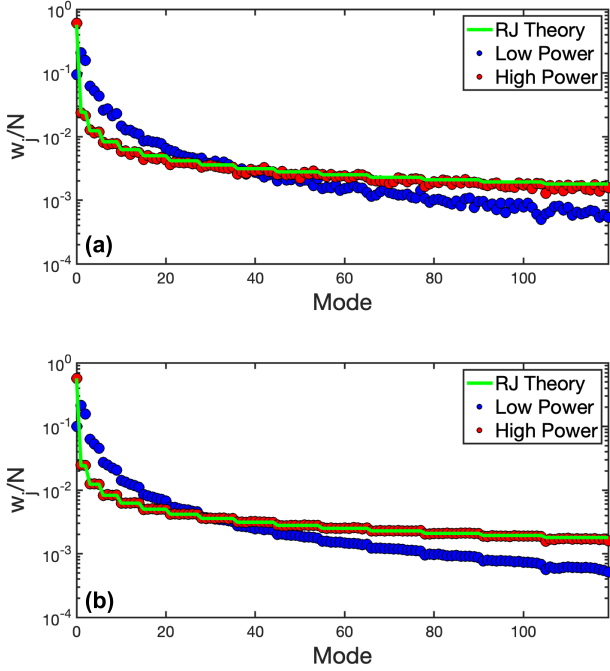


**FIG. S1: Observation of RJ thermalization (without disorder):** Experimental modal distributions  $w_j/N$  (circles), for an individual realization of the launched speckle beam (a), for an average over the realizations of speckle beams (b). The red circles report the results at high power ( $N = 7\text{kW}$ , nonlinear regime), and the blue circles at low power ( $N = 0.23\text{kW}$ , linear regime). The condensate fraction is  $w_0/N = 0.6$  for  $E/N = 1.94 \times 10^4 \text{m}^{-1}$  (a);  $w_0/N = 0.57$  for  $E/N = 2.05 \times 10^4 \text{m}^{-1}$  (b). Corresponding theoretical RJ equilibrium distribution  $w_j^{\text{RJ}}/N$  given from Eq.(S15) (green line): The quantitative agreement with the experimental data (red circles) is obtained without using any adjustable parameter.

$5 \times 10^3 \text{m}^{-1}$ ). The MMF guides  $M \simeq 120$  modes. The truncation of the potential introduces a frequency cut-off in the FF spectrum  $k_c = (2\pi/\lambda_0)\sqrt{n_{\text{co}}^2 - n_{\text{cl}}^2}$ . For details, see Supplementary Methods in Ref.[4].

The temporal spectrum was controlled by an optical spectrum analyzer (OSA) (600 to 1700nm range). The spectral analysis showed that the power scattered by self-stimulated Raman effect is in average  $\sim 5\%$  of the injected power. Also, the spectral analysis did not reveal the presence of parametric lines that would be induced by coupling between dispersive and nonlinear effects.

**2) Conservation of power  $N$  and energy  $E$  during propagation without strong disorder:** The conservation of the power has been verified by keeping fixed the conditions of injection of the speckle beam into the MMF: We measured  $N$  at the fiber output, and then at the input by cutting the fiber at 20cm, and we always obtained a relative power difference less than 1%. The conservation of the energy requires the NF and FF intensity measurements, which provide the potential energy  $E_{\text{pot}} = \int V(\mathbf{r})|\psi(\mathbf{r})|^2 d\mathbf{r}$ , and the kinetic energy  $E_{\text{kin}} = \int \alpha |\nabla\psi|^2 d\mathbf{r}$ , with  $E = E_{\text{kin}} + E_{\text{pot}}$ . The energy  $E_{\text{out}}$  is measured at the fiber output at  $L = 12\text{m}$ .

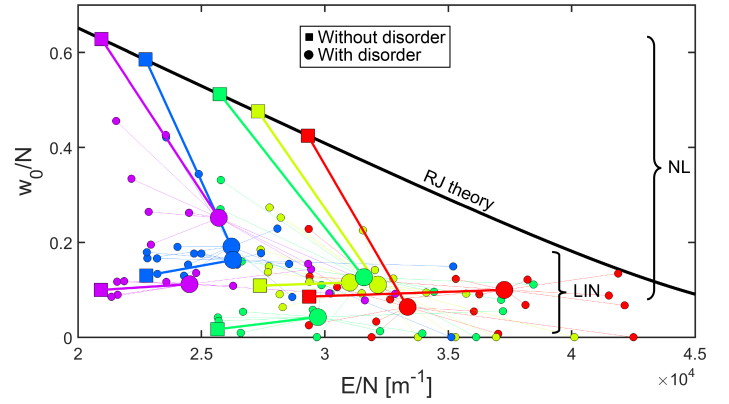


**FIG. S2: Suppression of light thermalization and condensation by strong disorder:** Measurements of the condensate fraction  $w_0/N$  vs energy  $E/N$  at small power (linear (LIN) regime) and high power (nonlinear (NL) regime), for a large strength of random mode coupling corresponding to an increase of the energy due to disorder of  $\Delta E/N \simeq 19\%$ . The black solid line reports the condensate fraction from the RJ theory,  $w_0^{\text{RJ}}/N$  vs  $E/N$ . In the absence of strong disorder (squares):  $w_0/N$  increases as the power increases, and reaches the value predicted by the RJ theory (solid line) – each color refers to a different value of the energy  $E/N$ . In the presence of strong disorder (big circles): the energy  $E/N$  increases (the squares are shifted to the big circles of the same color). The big circles report the average over 10 different realizations of disorder (10 small circles for each color). At variance with Fig. 4, here the strength of random mode coupling is so large that RJ thermalization and condensation are inhibited by strong disorder.

Without altering the fiber launch conditions, the fiber is cut to 20cm to get  $E_{\text{in}}$ . The procedure is repeated for different speckle beams (i.e., for different values of the energy  $E$ ), by moving the diffuser before injection into the MMF. We always obtained  $|E_{\text{out}} - E_{\text{in}}|/E_{\text{moy}} < 1\%$  for values of the energy that span the range of the condensation curve, i.e.  $w_0^{\text{RJ}}/N$  varying from 0 to 0.7.

**3) Experimental observation of RJ thermalization:** In the absence of strong disorder (i.e., absence of applied stress induced on the fiber), we observe the process of thermalization to the RJ equilibrium distribution,  $w_j^{\text{RJ}} = T/(\beta_j - \mu)$ . In the experiments, the modal populations ( $w_j$ ) are computed by using the Gerchberg-Saxton algorithm, which allows us to retrieve the transverse phase profile of the field from the NF and the FF intensity distributions measured in the experiments [5]. By projecting the complex field over the modes of the MMF (Gauss-Hermite basis) we get the complete modal distribution  $w_j/N$ ,  $j = 0, 1, \dots, M - 1$ . A typical example is reported in Fig. S1 showing the modal distribution  $w_j/N$  recorded experimentally at low-power (linear regime) and high-power (nonlinear regime), and its comparison to the RJ equilibrium distribution. Fig. S1(a) reports a single realization of the speckle beam, Fig. S1(b) reports an average over 60 realizations of speckle beams. The quantitative agreement between the experimental results and the theoretical RJ distribution is obtained without using adjustable parameters.

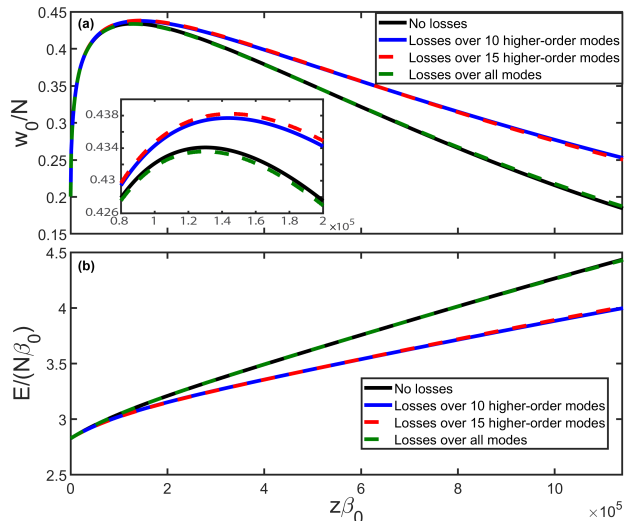


FIG. S3: **Impact of losses on the condensate fraction:** Simulation of the kinetic Eq.(S14) for the same parameters as Fig. 2 (main text): In the absence of losses (black), and when 10% of losses are distributed among all modes (dashed green), among the higher-order 10 modes of the fiber (blue), among the higher-order 15 modes of the fiber (dashed red). Condensate fraction  $w_0(z)/N(z)$  vs  $z$ , where  $N(z)$  is the local value of the power accounting for the losses (a), and corresponding evolutions of the energy  $E(z)/(N(z)\beta_0)$  (b). The inset in (a) shows a zoom: The condensate peak relevant to the experiments is only weakly affected by the presence of the losses.

#### 4) Experimental procedure with strong disorder (applied stress):

The laser beam is passed through a diffuser before injection of the speckle beam into the MMF. The coupling conditions and the position of the diffuser then fix the energy density  $E/N$  of the speckle beam. In the absence of applied stress,  $E/N$  is conserved through propagation in the MMF (see point 2) above). We report in Fig. 4(a) (main text), 5 different ensembles of measurements, each one corresponding to a fixed position of the diffuser (i.e. fixed value of the energy  $E/N$  without applied stress). For a given fixed position of the diffuser, we perform the following steps i)-vii) to retrieve 10 different realizations of disorder in Fig. 4(a):

**i)** Without applying any stress, we measure the NF and FF intensity patterns at high power ( $N = 7\text{kW}$ , nonlinear regime), and compute  $E/N$  and  $w_0/N$  (squares in Fig. 4(a)). We verify that  $w_0/N$  is in agreement with the value predicted by the RJ theory, see Ref.[4] for details.

**ii)** At low power ( $N = 0.23\text{kW}$ , linear regime) we measure

the NF and FF intensity patterns and compute  $E/N$  and  $w_0/N$ .

**iii)** We return to the previous higher power ( $N = 7\text{kW}$ , nonlinear regime) and we verify that we recover the same NF speckle beam as in step i).

**iv)** Then we apply stress to a specific location of the MMF. The stress is applied by using clamps mounted on a linear translation manual stage whose position is controlled at the micrometer scale. We adjust the amount of stress by measuring the power losses (10% in Fig. 4(a), corresponding to  $\Delta E/N \simeq 6\%$ ). Once the stress is adjusted, the power is increased up to the same average power of step i). We then measure the NF and FF intensity patterns and compute  $E/N$  and  $w_0/N$  (small circles in Fig. 4(a)).

**v)** In a next step we decrease the power ( $N = 0.23\text{kW}$ , linear regime), we measure the NF and FF intensity patterns and compute  $E/N$  and  $w_0/N$  (small circles in Fig. 4(a)).

**vi)** We return to the previous higher power ( $N = 7\text{kW}$ , nonlinear regime) and remove the applied stress. We verify that we recover the same initial NF speckle beam as in step i).

**vii)** We repeat the steps iv)-v)-vi) 10 times to get 10 different realizations of strong disorder (small circles). Each disorder realization is achieved by applying stress to a different position of the MMF by rotating the drum on which it is wound.

The procedure i)-vii) is repeated for a larger amount of applied stress (disorder), corresponding to an increase of energy due to disorder of  $\Delta E/N \simeq 11\%$  in Fig. 4(b) (20% of power losses), and  $\Delta E/N \simeq 19\%$  in Fig. S2 (40% of power losses). In Fig. S2 the strength of random mode coupling is so large that RJ thermalization and condensation are inhibited by strong disorder.

Note that losses induced by strong disorder only weakly affect the condensate fraction through the propagation in the MMF, as illustrated in the simulation reported in Fig. S3. We have considered 10% of losses (over the propagation length  $z\beta_0 = 11 \times 10^5$ ), in the case where losses are distributed homogeneously in mode space, and non-homogeneously in mode space (only the higher-order modes experience losses). We have considered the parameters of the simulation reported in Fig. 2 (main text), which refers to the most interesting regime where linear disorder effects and nonlinear effects are of the same order,  $\mathcal{L}_{\text{kin}}^{\text{RJ}} \lesssim \mathcal{L}_{\text{kin}}^{\text{eq}}$ . The condensate peak relevant to the experiments is only weakly affected by the losses, see the inset in Fig. S3(a). Note that, for larger propagation lengths, the losses concentrated on the higher-order modes reduce the effective number of modes and thus limit the increase of energy  $E/(N\beta_0)$  due to disorder (Fig. S3(b)), which in turn leads to an increase of the condensate fraction (Fig. S3(a)).

[1] J.-P. Fouque, J. Garnier, G. Papanicolaou, and K. Sølna, *Wave Propagation and Time Reversal in Randomly Layered Media* (Springer, 2007).  
[2] V.E. Zakharov, V.S. L'vov, G. Falkovich, *Kolmogorov Spectra of Turbulence I* (Springer, Berlin, 1992).

[3] I.S. Gradshteyn and I.M. Ryzhik, *Tables of Integrals, Sums, Series, and Products* (Academic Press, New York, 1980).  
[4] K. Baudin *et al.*, Phys. Rev. Lett. **125**, 244101 (2020).  
[5] J.R. Fienup, Applied Optics **21**, 2758 (1982).